

# Unified framework for efficiently computable quantum circuits

Igor Ermakov,<sup>1,2</sup> Oleg Lychkovskiy,<sup>3,2,1</sup> and Tim Byrnes<sup>4,5,6,7,\*</sup>

<sup>1</sup>*Department of Mathematical Methods for Quantum Technologies,*

*Steklov Mathematical Institute of Russian Academy of Sciences, 8 Gubkina St., Moscow 119991, Russia.*

<sup>2</sup>*Russian Quantum Center, Skolkovo, Moscow 143025, Russia.*

<sup>3</sup>*Skolkovo Institute of Science and Technology, Bolshoy Boulevard 30, bld. 1, Moscow 121205, Russia.*

<sup>4</sup>*New York University Shanghai, NYU-ECNU Institute of Physics at NYU Shanghai,*

*Shanghai Frontiers Science Center of Artificial Intelligence and Deep Learning,  
567 West Yangsi Road, Shanghai, 200126, China.*

<sup>5</sup>*State Key Laboratory of Precision Spectroscopy, School of Physical and Material Sciences,  
East China Normal University, Shanghai 200062, China*

<sup>6</sup>*Center for Quantum and Topological Systems (CQTS),*

*NYUAD Research Institute, New York University Abu Dhabi, UAE.*

<sup>7</sup>*Department of Physics, New York University, New York, NY 10003, USA*

(Dated: January 17, 2024)

Quantum circuits consisting of Clifford and matchgates are two classes of circuits that are known to be efficiently simulatable on a classical computer. We introduce a unified framework that shows in a transparent way the special structure that allows these circuits can be efficiently simulatable. The approach relies on analyzing the operator spread within a network of basis operators during the evolution of quantum circuit. Quantifying the complexity of a calculation by the number of operators with amplitude above a threshold value, we show that there is a generic form of the complexity curve involving an initial exponential growth, saturation, then exponential decay in the presence of decoherence. Our approach is naturally adaptable into a numerical procedure, where errors can be consistently controlled as a function of the complexity of the simulation.

*Introduction* Calculating the time dynamics of a quantum circuit on a classical computer is in general a difficult task [1–8]. This is most obviously seen in the discovery of numerous quantum algorithms [9–14], which have been shown to have speedups over their classical counterpart. In a quantum simulation context, this difficulty is closely related to the difficulty of calculating time dynamics of generic quantum many-body problems [15–19]. This difficulty is exploited of in the context of quantum computational advantage, where the task is to simulate time dynamics of a quantum system [5, 20–26]. In the seminal result by the Google collaboration, a quantum random circuit was used to show that equivalent results would be difficult to obtain using classical simulation [5]. Similarly, in boson sampling, photons enter a linear optical network, and the photonic detection probabilities are measured [2, 23, 27–30]; a task that is computationally difficult to simulate. In all these examples, the sequence of time evolutions of the quantum system — lacking any simplifying symmetry — makes classical prediction of the output a difficult task [7].

For qubit-based quantum circuits there are two notable exceptions to this. The first is the foundational result of Gottesman and Knill [31, 32], which states that any quantum circuit that consist only of Clifford gates can be efficiently computed classically. The second consist of circuits involving matchgates [33], which are defined as

any unitary operation of the form

$$U_M = \begin{pmatrix} a_{00} & 0 & 0 & a_{01} \\ 0 & b_{00} & b_{01} & 0 \\ 0 & b_{10} & b_{11} & 0 \\ a_{10} & 0 & 0 & a_{11} \end{pmatrix}, \quad (1)$$

where  $a_{ij}, b_{ij}$  with  $i, j \in \{0, 1\}$  are matrix elements of a  $2 \times 2$  unitary matrix with the same determinant. For a circuit consisting purely of matchgates on nearest neighbor qubits in a one dimensional geometry, and starting from a input state that is a product state, the expectation values in the computational basis can be calculated efficiently [33–36].

A natural question that occurs here is whether there is any connection between such efficiently simulatable circuits. This is potentially an important question as better understanding the structure of such efficiently simulatable circuits may provide additional tools to discover other such circuits. Even for circuits which are not efficiently simulatable in the general case, in certain circumstances the complexity may only grow slowly, making them tractable in certain regimes. Another way that a circuit may become effectively tractable is by the presence of decoherence and other imperfections. Advances in techniques in calculating the output of random quantum circuits in the presence of such imperfections have shown that this can reduce the computational complexity of simulating the output considerably [37, 38].

In this paper, we examine a generic sequence of unitary operations in a quantum circuit in the presence of decoherence that scales with the depth of the circuit (Fig.

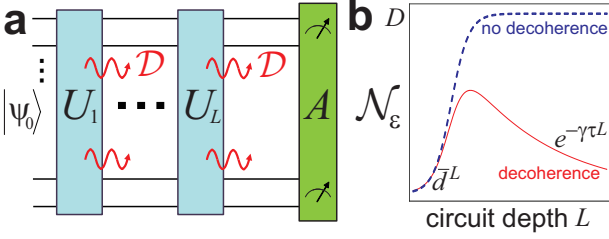


FIG. 1. (a) The problem considered in this paper. A sequence of  $L$  unitary gates  $U_l$  acts on an initial state  $|\psi_0\rangle$ . At the end, an observable  $A$  is measured. During each gate, some decoherence  $\mathcal{D}$  occurs, indicated by the wavy lines. (b) The generic evolution of the number of significant operators (12). In the absence of decoherence (dashed line), the number of operators increases exponentially and saturates. With decoherence, the number of operators initially increases exponentially but peaks and decays.

1(a)). We show a unified framework to understand both Clifford, matchgate, and other circuits which become effectively tractable. We study the complexity of simulating quantum dynamics in the context of operator growth. During the evolution, an initially local operator transforms into a superposition of numerous non-local operators in the Heisenberg picture, thereby increasing the computational cost. Recent studies have explored universal patterns of operator growth, linking it with out-of-time-order correlators and information scrambling in various systems [39–43]. It has been found that in open systems, dissipation competes with scrambling by restricting operator growth [44–47]. Yao and Schuster proposed a general framework for operator growth in open quantum systems[48], hypothesizing that, typically, operators with larger support decohere faster than local ones and can therefore be truncated. Polman et al. used a similar approach to develop a numerical tool for simulating energy and spin transport in several quantum many-body models [49]. However, such methods have not been applied to elucidate the connection between exactly solvable quantum circuits.

*Heisenberg evolution* Consider an  $N$ -qubit quantum circuit as shown in Fig. 1. The quantum circuit consists of a sequence of quantum gates consisting of  $L$  layers of unitaries  $U_l$  with  $l \in [1, L]$ . Each of the layers consist of a combination of gates that are choosable from a set  $\{u_i\}$ , where  $i$  labels all the possible gates that can be applied. For example, in the case of a Clifford circuit, this would be the Hadamard,  $S = e^{iZ\pi/4}$  phase, and CNOT gates, where  $Z$  is the Pauli matrix.

Suppose now we are interested in a particular observable  $A$  at the end of the circuit, such that we wish to know what  $\langle A \rangle$  is. Expand  $A$  in a complete orthonormal

operator basis  $B_k$

$$A = \sum_{k=1}^{4^N} \lambda_k B_k. \quad (2)$$

The  $\lambda_k$  are coefficients that may be computed by using the fact that  $\text{Tr}(B_j^\dagger B_k) = \delta_{jk}$ , such that  $\lambda_k = \text{Tr}(B_j^\dagger A)$ . A simple choice of an orthonormal operator basis are Pauli strings, i.e. tensor products of Pauli operators  $B_k = \otimes_{n=1}^N P_n / \sqrt{2^N}$  where  $P_n \in \{I_n, X_n, Y_n, Z_n\}$ .

First, consider a quantum circuit consisting of a single layer  $U$ , such that the gate depth is  $L = 1$ . The observable evolves in the Heisenberg picture as

$$A \rightarrow A' = U^\dagger A U = \sum_{k=1}^{4^N} \lambda_k B'_k. \quad (3)$$

Here we defined the evolved basis operator for the unitary  $U$  as

$$B'_k = U^\dagger B_k U = \sum_{j=1}^{4^N} \Omega_{jk} B_j \quad (4)$$

and expanded it using the operator basis with coefficients

$$\Omega_{jk} = \text{Tr}(B_j^\dagger U^\dagger B_k U). \quad (5)$$

Using this form, we see that the observable can be written as

$$A' = \sum_{j=1}^{4^N} \lambda'_j B_j, \quad (6)$$

where the new coefficients are

$$\lambda'_j = \sum_{k=1}^{4^N} \Omega_{jk} \lambda_k. \quad (7)$$

Repeating this process for  $L$  gates as shown in Fig. 1, we may obtain the final coefficients

$$\lambda'_j = \sum_{k_1, \dots, k_L=1}^{4^N} \Omega_{jk_1}^{(1)} \Omega_{k_1 k_2}^{(2)} \dots \Omega_{k_{L-1} k_L}^{(L)} \lambda_{k_L}. \quad (8)$$

This takes the form of a sequence of  $L$  square matrix multiplications each of dimension  $4^N \times 4^N$ .

In Eqs. (3) and (4) above, we only considered unitary evolution and did not take into account the decoherence. Taking into account of decoherence does not change the overall procedure, and may be written in the same formalism, where the  $\Omega^{(l)}$  matrices also includes the effect of decoherence. This is done by solving the Liouvillian equations of motion, and again expanding the result in the operator basis. We will generally consider a model of decoherence that is the same for all  $L$  layers (see Fig. 1(a)). Implicit in this structure is that the total amount of applied decoherence is proportional to the number of layers, which is typically the scenario in many quantum computing contexts as deep circuits take a longer evolution time. We give a simplified example of this below.

*Network representation* The product of the matrices  $\Omega = \Omega^{(1)}\Omega^{(2)}\dots\Omega^{(L)}$  contain all the information of how operators transform under a sequence of unitary evolutions. It is illuminating to see the structure of these transformations for several examples of quantum circuits. In Fig. 2, we visualize the matrix structure by interpreting  $|\Omega_{jk}|$  as elements of an adjacency matrix that encodes a directed graph. Here, the nodes of the graphs represent the  $4^N$  basis operators  $B_k$ , which we take as Pauli strings. The edges of the graphs represent the transformations that occur due to the action of the quantum circuit. In the case of the universal gate set of Clifford and  $T$  gates (Fig. 2(a)), we see a single connected graph (except the identity operator, which always appears as an isolated vertex), and no simple symmetry is apparent. This is in fact an example of a relatively sparse graph, with a mean vertex out-degree  $\bar{d} \approx 7.3$  for the case shown, and highest out-degree vertex  $d_{\max} = 16$ . For a completely random unitary, one would more typically have a fully connected graph, where  $\bar{d} \sim 4^N$ . For such a fully connected graph, the exponential number of operators generally means that the numerical simulation of the circuit is a difficult task, for this choice of basis operators. Meanwhile, for the case shown in Fig. 2(a), the sparsity suggests that some observables may be simulated effectively. For example, the observable  $X_3$  transforms to the single operator  $X_1X_2$  for the example shown. As the depth of the circuit is increased, the mean vertex degree increases, and the graph approaches a maximally connected graph, increasing the complexity of the circuit.

Contrast this to the graphs corresponding to a randomly chosen Clifford circuit as shown in Fig. 2(b). Clifford circuits simplify the graph structure considerably, such that they only consist of a single cycle, since Pauli strings transform to other Pauli strings. The mean vertex out-degree in this case is  $\bar{d} = 1$ , which is the key aspect for simulability of Clifford circuits. As long as one may keep track of the operator transformations at each step of the quantum circuit, one is able to compute the final full operator transformation. Unlike the universal gate circuit of Fig. 2(a) where the graph increases in connectivity, the single cycle structure remains independent of the depth  $L$ .

Figure 2(c) shows the graphs corresponding to a matchgate circuit. In this case, the simplifying aspect is that there are several disconnected graphs, such that the graph breaks into components (in addition to the trivial identity operator). This means that the matrix  $\Omega$  has a block diagonal structure. For each component, the vertices are fully connected, making them complete subgraphs. The right-most graph contains  $N^2$  vertices corresponding to operators known as Onsager strings, including all operators  $Z_n$ ,  $n \in [1, N]$  [50–53]. This allows for an efficient computation of the Heisenberg evolution of the operators due to the block diagonal structure of the evolution which avoids the full  $4^N$  operator space.

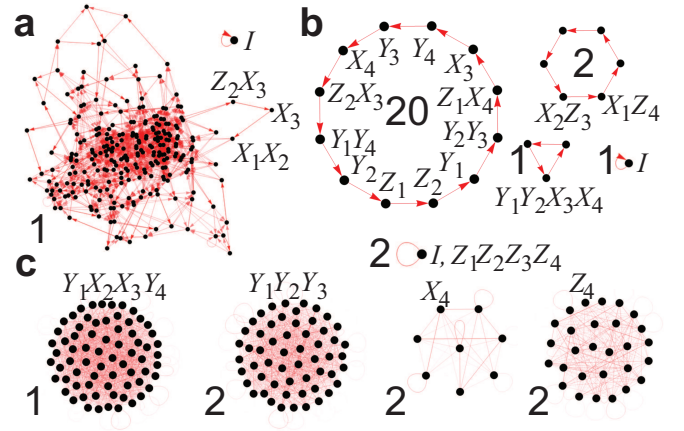


FIG. 2. Graphs corresponding to the adjacency matrix  $|\Omega_{jk}|$ . For each case we consider a  $N = 4$  qubit circuit with circuit depth  $L = 4$ . The gate sets chosen are (a) universal Clifford and  $T = e^{iZ\pi/8}$  gate; (b) Clifford; and (c) matchgate circuit. For (a)(b), each unitary  $U_l$  corresponds to a randomly selected single qubit and two qubit gate (including identity gates). Each graph node corresponds to a Pauli string, some of which are labeled. Large numbers indicate multiplicities of graphs with the same number of nodes and similar graphs (disregarding edge weights). The opacity of the edges are in proportion to the absolute value of the weight  $|\Omega_{lk}|$ .

The network picture provides a basis for understanding the computational difficulty of a given quantum circuit in the Heisenberg picture. Given an underlying graph structure of a quantum circuit, the observable transforms following graph edges and spreads throughout the network. Each successive application of a quantum gate then spreads through the network, such that more and more operators that must be kept account of, analogous to the spread of an epidemic. If the number of operators that must be accounted for increases exponentially, the simulation becomes intractable.

*Operator growth and decoherence.* The graphs shown in Fig. 2 correspond to operator transformations of the full quantum circuit. To see how the operators proliferate for deep quantum circuits, let us examine the spread of the operators throughout the network, layer by layer [54]. It will also be interesting to include decoherence at this point. As a simplified model of decoherence, we apply decoherence after each layer of gates, such that unitary and decoherence operations occur alternately. The general operator evolution under this type of evolution is

$$\lambda'_j = \sum_{k_1, \dots, k_L=1}^{4^N} \sum_{k'_1, \dots, k'_L=1}^{4^N} \Omega_{jk_1}^{(1)} \mathcal{D}_{k_1 k'_1} \dots \Omega_{k'_{L-1} k_L}^{(L)} \mathcal{D}_{k_L k'_L} \lambda_{k'_L}. \quad (9)$$

Here  $\mathcal{D}_{kk'}$  is the transformation associated with the decoherence process. To consider a specific case, let us choose Lindblad-Z dephasing on each qubit with rate  $\gamma$ . For an operator basis that is a Pauli string, the basis

operator evolves as  $B'_k = e^{-2\gamma q_k t} B_k$ , where  $t$  is the decoherence time of a single layer, and  $q_k$  is the number of  $X$  or  $Y$  Pauli matrices involved in  $B_k$  [53]. The transformation matrix is therefore diagonal and has elements  $\mathcal{D}_{kk'} = e^{-2\gamma q_k t} \delta_{kk'}$ .

In general, amplitudes of long Pauli strings tend to be suppressed by the decoherence [48, 49, 55]. To bound such suppression quantitatively, we assume that only one- and two-qubit gates are used. Then each unitary layer changes the length of a Pauli string at most by one Pauli matrix. If we count the layers in the reverse order (from right to left), then there are at least  $(q_k + 1 - l)$   $X$  and  $Y$  Pauli matrices in a Pauli string in the  $l$ th dissipative layer, adding the suppression factor  $e^{-2\gamma(q_k+1-l)t}$ . Multiplying these factors with  $l = 1, 2, \dots, q_k$  (we additionally assume that  $q_k \leq L$ ), one gets the bound

$$|\lambda'_k| \leq e^{-\gamma q_k(q_k-1)t} \|A\|. \quad (10)$$

An important quantity in the context of simulating such circuits in the Heisenberg picture is the number of operators that have a significant amplitude. We define an operator that has a significant amplitude as any coefficient in (6) that has an absolute value amplitude  $|\lambda'_l| \geq \epsilon$ , where  $\epsilon$  is a freely choosable cutoff parameter. Such definition is natural in the context of a numerical algorithm, where operators with amplitude less than the cutoff can be systematically truncated, at the expense of a loss in accuracy. The number of significant operators then has a definition

$$\mathcal{N}_\epsilon = \sum_{l=1}^{4^N} T_\epsilon(|\lambda'_l|), \quad (11)$$

where  $T_\epsilon(x) = \theta(x - \epsilon)$  is the threshold function, which is a displaced Heaviside step function.

Figure 3(a)-(c) shows  $\mathcal{N}_\epsilon$  for several types of random quantum circuits, each of depth  $L = 200$  chosen as specified with various rates of decoherence  $\gamma$  and threshold  $\epsilon$ . Figure 3(a) shows a universal Clifford +  $T$  gate circuit. Initially, we see an exponential growth  $\sim \bar{d}^L$  in the number of operators, consistent with the network epidemic picture. In the untruncated case ( $\epsilon = 0$ ) the growth in the number of operators occurs until it hits close to the maximum dimension  $4^N$  of the operator space. With truncation included, the number of operators is reduced, but remains constant without decoherence ( $\gamma = 0$ ). When decoherence is included, deep circuits reduce  $\mathcal{N}_\epsilon$  exponentially with  $L$ . We observe that the most difficult regions of simulation in a practical experiment therefore should occur somewhere in the middle of a deep quantum circuit, where exponential increase in the number of operators has occurred but decoherence has not set in completely.

Figure 3(b) shows  $\mathcal{N}_\epsilon$  for a random Clifford circuit. The number of operators always remains one, due to the

average vertex out-degree  $\bar{d} = 1$ , resulting in no exponential increase since  $\bar{d}^L = 1$ . With the onset of decoherence, for deep enough circuits the single operator even becomes unnecessary to keep track of and  $\mathcal{N}_\epsilon$  drops to zero, indicating all expectation values are close to zero. Figure 3(c) shows the case for a matchgate circuit. Here, the growth of  $\mathcal{N}_\epsilon$  is immediate due to the maximal connections in the graph of operators in the  $Z_L$  sector as seen in Fig. 2(c). This maximal value is however considerably smaller than in Fig. 2(a) due to the disconnected graph structure. The number of significant operators then drops exponentially allowing for the possibility to truncate operators and thereby further save resources for deep circuits.

Using this network approach to evaluating quantum circuits, we obtain the schematic complexity of a circuit. This can be described by an empirical relation (Fig. 1(b))

$$\mathcal{N}_\epsilon \propto \frac{De^{-\epsilon\gamma\tau L}\bar{d}^L}{D - 1 + a\bar{d}^L}, \quad (12)$$

where  $D$  is the order of the graph in question and  $\bar{d}$  is the mean vertex out-degree *per layer* characterizing the growth of the operators, and  $\tau, a$  are constants. Initially there is an exponential increase in the complexity of the circuit. Without decoherence, this increase eventually saturates, bounded by the order of graph, which is the full operator space dimension  $D = 4^N$  in the general case of a universal circuit, or at a lower level in the case symmetries are present as with matchgates. When decoherence is present, there is an exponential decay, as various operators start to degrade at different rates. All the graphs of Fig. 3(a)-(c) agree with the relation (12).

We note that our procedure is directly adaptable into a approximate numerical algorithm. Figure 3(d) shows the expectation value of  $Z_N$  including decoherence for the same quantum circuit as in Fig. 3(a), comparing the full calculation ( $\epsilon = 0$ ) with the truncated version ( $\epsilon = 0.01$ ). We see that there is excellent agreement for all times. The difference between the two curves (inset of Fig. 3(d)) remains a constant value of the order of  $\epsilon$ , as expected as we have systematically truncated operators with amplitudes less than  $\epsilon$ . Note that considering the full calculation requires a number of operators for  $\epsilon = 0$  that is far greater than the truncated curves, as shown in Fig. 3(a).

*Basis choice* The structure of the matrix  $\Omega$  is highly dependent upon the choice of basis operators  $B_k$ . Pauli strings are merely a convenient choice and other bases may be chosen, which potentially simplifies the graph structure. In the sense of obtaining the simplest possible graphs, the optimal basis choice is attained by using the eigenvectors of the  $\Omega$  matrix, which completely diagonalizes it as  $V^\dagger \Omega V = \Lambda$ . Here  $V$  is a unitary matrix and  $\Lambda$  is a diagonal matrix containing the eigenvalues of  $\Omega$ . The eigenvalues are complex numbers  $e^{-i(E_n - E_m)t}$ . This originates from the fact that in this basis, the transformed basis operators take the form  $\tilde{B}_{nm} = |E_n\rangle\langle E_m|$ , where

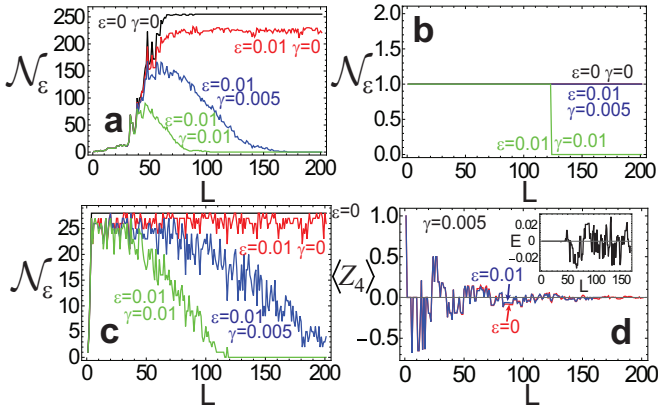


FIG. 3. (a)-(c) The number of significant operators for various quantum circuits with  $N = 4$  as measured by the number of significant operators (11). Quantum circuits correspond to (a) Clifford + T gate; (b) Clifford; (c) matchgates. The three lines marked by  $\gamma$  have a truncation parameter of  $\epsilon = 0.01$ . The line marked as  $\epsilon = 0$  is full number of operators with  $\gamma = 0$  for comparison. In each circuit, the gates are chosen randomly, but are kept consistent for different parameters  $\gamma, \epsilon$ . (d) Expectation value of  $Z_N$  for the same circuit as in (a) with  $\gamma = 0.005$  and  $\epsilon$  as marked. The initial state is chosen as  $|0\rangle^{\otimes N}$ . Inset shows the difference between the two curves  $E = \langle Z_4 \rangle_{\epsilon=0.01} - \langle Z_4 \rangle_{\epsilon=0}$ . The observable  $A = Z_N$  is chosen for all cases, the decoherence time is  $t = 1$ .

$|E_n\rangle$  are the eigenstates of the effective Hamiltonian of the unitary evolution of the quantum circuit  $U = e^{-iH_{\text{eff}}t}$ . The implication of this is that by choosing an improved operator basis, it is possible to simplify the network, in this case to  $4^N$  disconnected single vertices (an empty graph).

*Conclusions* We have shown that it is possible to understand several efficiently simulatable quantum circuits, specifically the Clifford and matchgate quantum circuits in terms of a single framework. While conventionally these circuits are understood in terms of the stabilizer formalism and fermionic transformations, our approach uses a simple Heisenberg picture of operators and analyzes the operator connectivity in a graph theoretical framework. The key picture is that the quantum circuit can be equivalently thought of as a proliferation of operators through a network of basis operators. Eq. (12) captures the relevant ingredients that determine whether a particular observable is tractable or not. There is an interplay of the vertex out-degree, graph component structure, and decoherence which affects the simulability of a circuit. In the network picture, decoherence reduces the number of active nodes in the network, which helps to contain the spread to all operators. Our approach is adaptable into a classical algorithm, by keeping only those operators with a significant amplitude. By choosing an efficient operator basis it is always possible to reduce the complexity, in the ideal case to an empty graph. While finding such a basis is in general a difficult task, even a partial reduction of

the graph degree should be highly beneficial to reduce the complexity, which would be beneficial in the context of a numerical algorithm.

This work is supported by the National Natural Science Foundation of China (62071301); NYU-ECNU Institute of Physics at NYU Shanghai; Shanghai Frontiers Science Center of Artificial Intelligence and Deep Learning; the Joint Physics Research Institute Challenge Grant; the Science and Technology Commission of Shanghai Municipality (19XD1423000,22ZR1444600); the NYU Shanghai Boost Fund; the China Foreign Experts Program (G2021013002L); the NYU Shanghai Major-Grants Seed Fund; Tamkeen under the NYU Abu Dhabi Research Institute grant CG008; and the SMEC Scientific Research Innovation Project (2023ZKZD55).

\* tim.byrnes@nyu.edu

- [1] R. P. Feynman *et al.*, Simulating physics with computers, *Int. j. Theor. phys.* **21** (2018).
- [2] S. Aaronson and A. Arkhipov, The computational complexity of linear optics, in *Proceedings of the forty-third annual ACM symposium on Theory of computing* (2011) pp. 333–342.
- [3] M. J. Bremner, R. Jozsa, and D. J. Shepherd, Classical simulation of commuting quantum computations implies collapse of the polynomial hierarchy, *Proceedings of the Royal Society A: Mathematical, Physical and Engineering Sciences* **467**, 459 (2011).
- [4] M. J. Bremner, A. Montanaro, and D. J. Shepherd, Achieving quantum supremacy with sparse and noisy commuting quantum computations, *Quantum* **1**, 8 (2017).
- [5] F. Arute, K. Arya, R. Babbush, D. Bacon, J. C. Bardin, R. Barends, R. Biswas, S. Boixo, F. G. Brandao, D. A. Buell, *et al.*, Quantum supremacy using a programmable superconducting processor, *Nature* **574**, 505 (2019).
- [6] S. Boixo, S. V. Isakov, V. N. Smelyanskiy, R. Babbush, N. Ding, Z. Jiang, M. J. Bremner, J. M. Martinis, and H. Neven, Characterizing quantum supremacy in near-term devices, *Nature Physics* **14**, 595 (2018).
- [7] A. Bouland, B. Fefferman, C. Nirkhe, and U. Vazirani, On the complexity and verification of quantum random circuit sampling, *Nature Physics* **15**, 159 (2019).
- [8] R. Movassagh, The hardness of random quantum circuits, *Nature Physics* **19**, 1 (2023).
- [9] M. A. Nielsen and I. Chuang, *Quantum computation and quantum information* (2002).
- [10] P. W. Shor, Algorithms for quantum computation: discrete logarithms and factoring, in *Proceedings 35th annual symposium on foundations of computer science* (Ieee, 1994) pp. 124–134.
- [11] L. K. Grover, A fast quantum mechanical algorithm for database search, in *Proceedings of the twenty-eighth annual ACM symposium on Theory of computing* (1996) pp. 212–219.
- [12] A. W. Harrow, A. Hassidim, and S. Lloyd, Quantum algorithm for linear systems of equations, *Phys. Rev. Lett.* **103**, 150502 (2009).

- [13] M. Mosca, Quantum algorithms, arXiv preprint arXiv:0808.0369 (2008).
- [14] L. Tessler and T. Byrnes, Bitcoin and quantum computing, arXiv preprint arXiv:1711.04235 (2017).
- [15] S. Lloyd, Universal quantum simulators, *Science* **273**, 1073 (1996).
- [16] J. Eisert, M. Friesdorf, and C. Gogolin, Quantum many-body systems out of equilibrium, *Nature Physics* **11**, 124 (2015).
- [17] A. Smith, M. Kim, F. Pollmann, and J. Knolle, Simulating quantum many-body dynamics on a current digital quantum computer, *npj Quantum Information* **5**, 106 (2019).
- [18] D. Bluvstein, A. Omran, H. Levine, A. Keesling, G. Semeghini, S. Ebadi, T. T. Wang, A. A. Michailidis, N. Maskara, W. W. Ho, *et al.*, Controlling quantum many-body dynamics in driven rydberg atom arrays, *Science* **371**, 1355 (2021).
- [19] P. Schindler, M. Müller, D. Nigg, J. T. Barreiro, E. A. Martinez, M. Hennrich, T. Monz, S. Diehl, P. Zoller, and R. Blatt, Quantum simulation of dynamical maps with trapped ions, *Nature Physics* **9**, 361 (2013).
- [20] J. Preskill, Quantum computing and the entanglement frontier, arXiv preprint arXiv:1203.5813 (2012).
- [21] A. P. Lund, M. J. Bremner, and T. C. Ralph, Quantum sampling problems, bosonsampling and quantum supremacy, *npj Quantum Information* **3**, 15 (2017).
- [22] D. Hangleiter and J. Eisert, Computational advantage of quantum random sampling, *Reviews of Modern Physics* **95**, 035001 (2023).
- [23] H.-S. Zhong, H. Wang, Y.-H. Deng, M.-C. Chen, L.-C. Peng, Y.-H. Luo, J. Qin, D. Wu, X. Ding, Y. Hu, *et al.*, Quantum computational advantage using photons, *Science* **370**, 1460 (2020).
- [24] Y. Wu, W.-S. Bao, S. Cao, F. Chen, M.-C. Chen, X. Chen, T.-H. Chung, H. Deng, Y. Du, D. Fan, *et al.*, Strong quantum computational advantage using a superconducting quantum processor, *Physical review letters* **127**, 180501 (2021).
- [25] L. S. Madsen, F. Laudenbach, M. F. Askarani, F. Rortais, T. Vincent, J. F. Bulmer, F. M. Miatto, L. Neuhaus, L. G. Helt, M. J. Collins, *et al.*, Quantum computational advantage with a programmable photonic processor, *Nature* **606**, 75 (2022).
- [26] Q. Zhu, S. Cao, F. Chen, M.-C. Chen, X. Chen, T.-H. Chung, H. Deng, Y. Du, D. Fan, M. Gong, *et al.*, Quantum computational advantage via 60-qubit 24-cycle random circuit sampling, *Science bulletin* **67**, 240 (2022).
- [27] M. A. Broome, A. Fedrizzi, S. Rahimi-Keshari, J. Dove, S. Aaronson, T. C. Ralph, and A. G. White, Photonic boson sampling in a tunable circuit, *Science* **339**, 794 (2013).
- [28] J. B. Spring, B. J. Metcalf, P. C. Humphreys, W. S. Kolthammer, X.-M. Jin, M. Barbieri, A. Datta, N. Thomas-Peter, N. K. Langford, D. Kundys, *et al.*, Boson sampling on a photonic chip, *Science* **339**, 798 (2013).
- [29] M. Tillmann, B. Dakić, R. Heilmann, S. Nolte, A. Szameit, and P. Walther, Experimental boson sampling, *Nature photonics* **7**, 540 (2013).
- [30] C. S. Hamilton, R. Kruse, L. Sansoni, S. Barkhofen, C. Silberhorn, and I. Jex, Gaussian boson sampling, *Physical review letters* **119**, 170501 (2017).
- [31] D. Gottesman, The heisenberg representation of quantum computers, arXiv preprint quant-ph/9807006 (1998).
- [32] S. Aaronson and D. Gottesman, Improved simulation of stabilizer circuits, *Physical Review A* **70**, 052328 (2004).
- [33] L. G. Valiant, Expressiveness of matchgates, *Theoretical Computer Science* **289**, 457 (2002).
- [34] L. G. Valiant, Quantum computers that can be simulated classically in polynomial time, in *Proceedings of the thirty-third annual ACM symposium on Theory of computing* (2001) pp. 114–123.
- [35] R. Jozsa and A. Miyake, Matchgates and classical simulation of quantum circuits, *Proceedings of the Royal Society A: Mathematical, Physical and Engineering Sciences* **464**, 3089 (2008).
- [36] D. J. Brod, Efficient classical simulation of matchgate circuits with generalized inputs and measurements, *Physical Review A* **93**, 062332 (2016).
- [37] D. Aharonov, X. Gao, Z. Landau, Y. Liu, and U. Vazirani, A polynomial-time classical algorithm for noisy random circuit sampling, in *Proceedings of the 55th Annual ACM Symposium on Theory of Computing* (2023) pp. 945–957.
- [38] J. Shi and T. Byrnes, Effect of partial distinguishability on quantum supremacy in gaussian boson sampling, *npj Quantum Information* **8**, 54 (2022).
- [39] A. Nahum, S. Vijay, and J. Haah, Operator spreading in random unitary circuits, *Physical Review X* **8**, 021014 (2018).
- [40] C. W. von Keyserlingk, T. Rakovszky, F. Pollmann, and S. L. Sondhi, Operator hydrodynamics, otocs, and entanglement growth in systems without conservation laws, *Physical Review X* **8**, 021013 (2018).
- [41] D. E. Parker, X. Cao, A. Avdoshkin, T. Scaffidi, and E. Altman, A universal operator growth hypothesis, *Physical Review X* **9**, 041017 (2019).
- [42] X. Mi, P. Roushan, C. Quintana, S. Mandra, J. Marshall, C. Neill, F. Arute, K. Arya, J. Atalaya, R. Babbush, *et al.*, Information scrambling in quantum circuits, *Science* **374**, 1479 (2021).
- [43] K. A. Landsman, C. Figgatt, T. Schuster, N. M. Linke, B. Yoshida, N. Y. Yao, and C. Monroe, Verified quantum information scrambling, *Nature* **567**, 61 (2019).
- [44] V. Khemani, A. Vishwanath, and D. A. Huse, Operator spreading and the emergence of dissipative hydrodynamics under unitary evolution with conservation laws, *Physical Review X* **8**, 031057 (2018).
- [45] Y.-L. Zhang, Y. Huang, X. Chen, *et al.*, Information scrambling in chaotic systems with dissipation, *Physical Review B* **99**, 014303 (2019).
- [46] A. Touil and S. Deffner, Information scrambling versus decoherence—two competing sinks for entropy, *PRX Quantum* **2**, 010306 (2021).
- [47] B. Yoshida and N. Y. Yao, Disentangling scrambling and decoherence via quantum teleportation, *Physical Review X* **9**, 011006 (2019).
- [48] T. Schuster and N. Y. Yao, Operator growth in open quantum systems, *Phys. Rev. Lett.* **131**, 160402 (2023).
- [49] T. Rakovszky, C. W. von Keyserlingk, and F. Pollmann, Dissipation-assisted operator evolution method for capturing hydrodynamic transport, *Phys. Rev. B* **105**, 075131 (2022).
- [50] M. Znidaric, Exact solution for a diffusive nonequilibrium steady state of an open quantum chain,

Journal of Statistical Mechanics: Theory and Experiment **2010**, [h0X0023\(2010\)155](https://doi.org/10.1088/1742-5468/2010/03/155) (2023).

[51] N. Shibata and H. Katsura, Dissipative spin chain as a non-Hermitian Kitaev ladder, Phys. Rev. B **99**, 174303 (2019).

[52] F. H. L. Essler and L. Piroli, Integrability of one-dimensional lindbladians from operator-space fragmentation, Phys. Rev. E **102**, 062210 (2020).

[53] A. Teretenkov and O. Lychkovskiy, Exact quantum dynamics of selected observables in integrable and non-integrable open many-body systems, arXiv preprint

[54] D. E. Parker, X. Cao, A. Avdoshkin, T. Scaffidi, and E. Altman, A universal operator growth hypothesis, Phys. Rev. X **9**, 041017 (2019).

[55] D. Wellnitz, G. Preisser, V. Alba, J. Dubail, and J. Schachenmayer, Rise and fall, and slow rise again, of operator entanglement under dephasing, Phys. Rev. Lett. **129**, 170401 (2022).